Extracellular Protons Inhibit the Activity of Inward-Rectifying Potassium Channels in the Motor Cells of *Samanea saman* Pulvini[1]

Ling Yu, Menachem Moshelion, and Nava Moran*

Department of Agricultural Botany, Institute of Plant Sciences and Genetics in Agriculture, Faculty of Agricultural, Food, and Environmental Quality Sciences, The Hebrew University of Jerusalem, Rehovot 76100, Israel

The intermittent influx of K^+ into motor cells in motor organs (pulvini) is essential to the rhythmic movement of leaves and leaflets in various plants, but in contrast to the K^+ influx channels in guard cells, those in pulvinar motor cells have not yet been characterized. We analyzed these channels in the plasma membrane of pulvinar cell protoplasts of the nyctinastic legume *Samanea saman* using the patch-clamp technique. Inward, hyperpolarization-activated currents were separated into two types: time dependent and instantaneous. These were attributed, respectively, to K^+-selective and distinctly voltage-dependent K_H channels and to cation-selective voltage-independent leak channels. The pulvinar K_H channels were inhibited by external acidification (pH 7.8–5), in contrast to their acidification-promoted counterparts in guard cells. The inhibitory pH effect was resolved into a reversible decline of the maximum conductance and an irreversible shift of the voltage dependence of K_H channel gating. The leak appeared acidification insensitive. External Cs (10 mM in 200 mM external K^+) blocked both current types almost completely, but external tetraethylammonium (10 mM in 200 mM external K^+) did not. Although these results do not link these two channel types unequivocally, both likely serve as K^+ influx pathways into swelling pulvinar motor cells. Our results emphasize the importance of studying multiple model systems.

Motor cells such as stomatal guard cells or flexors and extensors of the leaf-moving organs (pulvini) increase their volume and turgor mainly due to the uptake of K^+ and Cl^-. Signals causing the motor cell swelling and increase of turgor activate the plasma membrane H^+ pump, leading to hyperpolarization in guard cells (Assmann et al., 1985) and in pulvini (Racusen and Satter, 1975; Kim et al., 1992, 1993), and to the acidification of the apoplast in guard cells (Shimazaki et al., 1985; Edwards et al., 1988) and in pulvini (Iglesias and Satter, 1983; Erath et al., 1988; Lee and Satter, 1989; Starrach and Meyer, 1989). The swelling signals and the hyperpolarization also activate K^+ influx in guard cells (Humble and Rashke, 1971; Blatt, 1985; Bowling, 1987) and in pulvini (Lowen and Satter, 1989; Starrach and Meyer, 1989; Kim et al., 1992, 1993). The influx of K^+ occurs via K^+-selective, inward-rectifying K channels activated by hyperpolarization (K_{in}, or K_H channels) in guard cells (Schroeder et al., 1987; Schroeder, 1988; Blatt, 1992; Ilan et al., 1996) and in pulvini (Moran, 1990).

The function and regulation of K_H (K_{in}) channels in guard cells has been described extensively (Schroeder, 1988, 1995; Fairley-Grenot and Assmann, 1992b, 1993). They are activated by acidification (Blatt, 1992; Ilan et al., 1996; Dietrich et al., 1998), blocked by Ca^{2+} (Schroeder and Hagiwara, 1989; Blatt, 1992; Fairley-Grenot and Assmann, 1992a; Lemtiri-Chlieh and MacRobbie, 1994; Kelly, 1995; Dietrich et al., 1998; Grabov and Blatt, 1999), and they depend on external K^+ (Schroeder, 1988; Blatt, 1992). These are by far the best characterized native plant K channels. The characterization of these K_H (K_{in}) channels includes their molecular identification with the widely studied KAT1 channel and its close homologs (Schachtman et al., 1992; Cao et al., 1995; Hoshi, 1995; Nakamura et al., 1995; Becker et al., 1996; Hoth et al., 1997b; Ichida et al., 1997; Li et al., 1998; Uozumi et al., 1998; Baizabal-Aguirre et al., 1999; Bruggemann et al., 1999; Tang et al., 2000; for review, see Czempinski et al., 1999; Dreyer et al., 1999; Zimmermann and Sentenac, 1999).

In contrast to guard cells, there is no comparable information (except for a brief report; see Moran, 1990) on the K^+ influx channels of the pulvinar motor cells. On the contrary, various attempts to activate them in *Mimosa pudica* failed (H. Stoeckel, personal communication). Neither have any records been published as yet of inward K^+ currents in the *Phaseolus* pulvini. We are presenting here the first characterization of K^+ influx channels from motor cells of pulvini of the legume *Samanea saman*, of the *Mimosa*

[1] This work was supported by The German-Israeli Foundation for Scientific Research and Development (grant no. G 193–207.02/94 to N.M.), by The United States-Israel Binational Agricultural Research and Development Fund (grant no. IS–2469–94CR), and by Dead-Sea Works Ltd., Israel.

* Corresponding author; e-mail nava.moran@huji.ac.il; fax 972–8–946–7763.

Article, publication date, and citation information can be found at www.plantphysiol.org/cgi/doi/10.1104/pp.010335.

family. In accordance with the presumably identical roles of K^+ influx channels in the swelling of the motor cells (for review, see Satter and Galston, 1981; Freudling et al., 1988; Moran, 1990), we expected the K_H channels in both cell types to behave similarly. However, in a surprising contrast to guard cell K_H channels activated by extracellular acidification, the K_H channels of *S. saman* pulvini were inhibited by external protons. These contrasting results emphasize the importance of studying channels in a variety of model systems, in preference to focusing on a single cell type.

RESULTS

Instantaneous versus Time-Dependent Currents

Voltage Dependence of Inward Currents

Hyperpolarization of motor cell protoplasts, "patch clamped" in a whole-cell configuration and bathed in a solution containing 40 or 200 mM K^+, elicited inward currents (Fig. 1). These consisted of an instantaneous inward current response and, at larger hyperpolarizations, a time-dependent inward current that, during each 4-s voltage pulse, increased gradually toward a steady state. To compare the voltage dependence of the instantaneous and the time-dependent currents, we examined the I-V relationships of cells with the larger currents (setting the threshold for the time-dependent currents at −170 mV arbitrarily at −25 pA). The amplitudes of the instantaneous current and the time-dependent current in these cells increased with the degree of the hyperpolarization, although with a different voltage dependence. The current-voltage (I-E_M) relationship of the time-dependent currents was very nonlinear (Fig. 1B), in contrast to the nearly linear I-E_M relationship of the instantaneous currents (Fig. 1C). At 200 mM, the mean time-dependent current (at −170 mV) was nearly 3-fold larger than at 40 mM (Fig. 1B). The instantaneous current also increased considerably, often necessitating on-line subtraction (Fig. 1C; see "Materials and Methods").

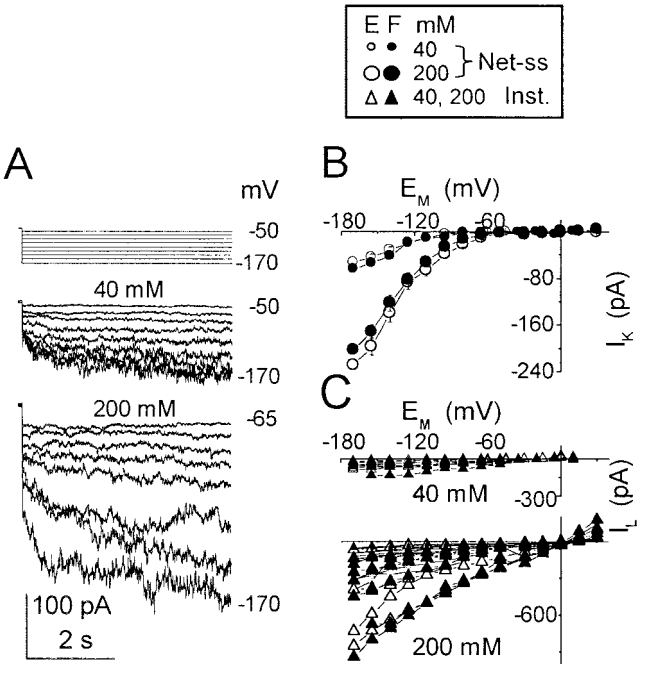

Figure 1. Two types of inward currents at two concentrations of external K^+. A, Pulse protocol (top) elicited inward currents from a flexor cell at the indicated $[K^+]_O$ (superimposed records, middle and bottom). Numbers at the right are the membrane potentials during the corresponding pulses. (f), Pipette solution. B, I-E_M relationships of the time-dependent currents (mean ± SE) from extensors (E) and flexors (F). At $[K^+]_O$ of 40 mM, the mean values of current at −170 mV were −53 ± 9 (± SE, $n = 6$) in E and −64 ± 16 pA ($n = 5$) in F; at 200 mM, 203 ± 31 pA ($n = 11$) in E and 229 ± 36 ($n = 12$) in F. Note the much smaller error bars due to the normalization procedure (if not seen, the errors are smaller than the symbols; see "Materials and Methods" for details). The following combinations of bath/pipette solutions were used (see "Materials and Methods" for details): bath: 40 mM K^+ (solution b)/pipette: (solution f), or (h) or (g), or bath: 200 mM K^+ (solution c)/pipette: (f). C, I-E_M relationships of the instantaneous currents from individual cells of B.

Selectivity

Due to the automatic subtraction of the holding currents at external $[K^+]$ ($[K^+]_O$) of 200 mM in some of the experiments, the zero crossover points of the I-E_M curves (the "reversal potentials") of the instantaneous current cannot attest to the selectivity (or lack thereof) of this current at 200 mM. Also, because of the differences in their zero crossover points, the I-E_M curves are presented here without averaging. It should be emphasized, however, that due to the fact that this subtraction shifted each cell's I-E_M curves of the instantaneous and the time-dependent currents identically (upwardly), the determination of the reversal potentials, E_{rev}s, of the time-dependent currents at 200 mM remains valid (see "Materials and Methods"). No such subtraction was performed at $[K^+]_O$ of 40 mM, and therefore at this concentration E_{rev} values could be determined unambiguously for both types of currents.

Between 40 and 200 mM K^+ in the bath and with 137 to 157 mM K^+ inside the cell, the E_{rev} of the time-dependent current (determined as described in "Materials and Methods") did not differ significantly from E_K, the Nernst potential of K^+ (Fig. 2, dotted line). The calculated E_K values were: −80 mV [for solutions (a)/(f)], between −29 and −32 mV [for solutions (b)/(f) to (b)/(h), respectively], or 9 mV [solutions (c)/(f)]. The Nernst potentials for other ions were: E_{Cl}, +27 mV or −10 mV [with (b) or (c) solutions outside, respectively]; E_H, 0 mV or +106 mV (with external pH 7.8 or 6.0, respectively); and E_{Ca}, between 163 and 172 mV [with internal solutions (f) to (h), respectively, and 0.3 mM Ca^{2+} in the bath], or between 133 and 147 mV [with (f) and (h), respectively, and with 1 mM Ca^{2+} in the bath].

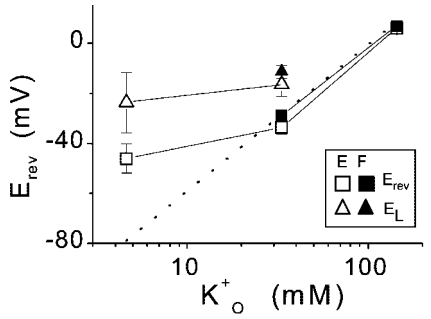

Figure 2. Reversal potentials of the inward currents. Mean values (± SE) of E_{rev} and E_L, the reversal potentials of the time-dependent and the instantaneous currents, versus K^+_O, K^+ activity in the bath. K^+_O was calculated from the external K^+ concentrations using activity coefficients from (Robinson and Stokes, 1965). When not seen, the error bars are smaller than the symbols. Data are from four extensors (E) at $[K^+]_O$ of 5 mM, five extensors, and eight flexors (F) at 40 mM and from 10 extensors and 11 flexors at 200 mM. The dotted line represents the calculated E_K, the Nernst potential of K^+ (Eq. 2). Solutions were distributed as follows: bath: 5 mM K^+ (solution a)/pipette: (f); bath: 40 mM K^+ (solution b)/pipette: (f) (four extensors and six flexors), or (g) (one flexor), or (h) (one extensor and one flexor); bath: 200 mM K^+ solution c)/pipette: (f).

At an external K^+ concentration of 40 mM, E_{rev} was markedly different from the reversal potential of the instantaneous current, E_L. This difference was particularly striking when examined on a cell-to-cell basis. Thus, the paired differences between E_{rev} and E_L (determined in each cell separately), averaged over five extensors and eight flexors, were significantly different from zero (these differences were, respectively, -17 ± 5 mV [$P < 0.02$] and -17 ± 2 mV [$P < 0.01$]). This disparity between the reversal potentials of the time-dependent current and the instantaneous current (Fig. 2) indicates a significant difference in the K^+ selectivity of the two pathways. It is very likely that in addition to K^+, the instantaneous current pathway was markedly permeable also to Cl^- or to H^+ and/or to Ca^{2+}. Based on this lack of K^+ specificity, we term the instantaneous current "leak" (I_L). In contrast to I_L, at $[K^+]_O$ of 40 mM, the hyperpolarization-activated, time-dependent current pathway was highly K^+ selective (relatively to other ions in the experimental solutions) not only in comparison with the instantaneous current pathway(s), but also in absolute terms (Fig. 2). Thus, we term the time-dependent current I_K and attribute it to K_H channels (hyperpolarization-activated K channels).

With 5 mM K^+ and 1 mM Ca^{2+} in the bath, in extensors, both types of pathways were far from ideally K^+ selective; whereas E_K was -80 mV, the mean E_{rev} value was -46 ± 6 mV ($n = 4$; Fig. 2). This low apparent K^+ selectivity of the whole-cell membrane at $[K^+]_O$ of 5 mM may be explained by the small contribution of specific K_H channels relatively to other time-dependent ionic pathways under these conditions. Notwithstanding this low K_H channel selectivity, the disparity between E_{rev} and E_L was still considerable ($P < 0.02$); when examined in pairs separately in each cell, the mean difference amounted to 23 ± 6 mV.

Effects of Tetraethylammonium (TEA) and Cs^+ on the Inward Currents

Block by TEA and Cs^+ is a widely used tool for the identification of channels. In our experiments, the inward currents in five cells (two extensors and three flexors) were not affected by TEA added to the bath (at a final concentration of 10 mM in the presence of 200 external mM K^+), I_L was inhibited by 8% ± 15% (mean ± SE), and I_K was inhibited by 19% ± 12% (data not shown). In contrast, in three cells (flexors), adding Cs^+ (final concentration of 10 mM in the presence of 200 mM external K^+) blocked both currents similarly ($P < 0.05$): I_L by 66% ± 14% and I_K by 93% ± 7% (Fig. 3), strongly suggesting that the leak channel is also a K channel.

Correlation between the Two Types of Conduits

If I_K and I_L flow via the same conduit, as has been hypothesized for one type of plant inward-rectifying K channel, the AKT2 channel (Marten et al., 1999), their amplitudes should depend similarly on the number of conduits in a cell, and therefore, they should be positively correlated when compared on a cell-to-cell basis. At $[K^+]_O$ of 5 and 40 mM, we examined this correlation between I_K and I_L at -170 mV, extracted in pairs separately from each one of 30 randomly picked cells at each K^+ concentration, without any a priori criteria for current amplitudes (Fig. 4, A–D). At $[K^+]_O$ of 200 mM, we examined the correlation between the conductances corresponding to I_K and I_L, rather than between I_K and I_L themselves, because of the automatic correction for I_L (see "Materials and Methods"; notably, this correction did not

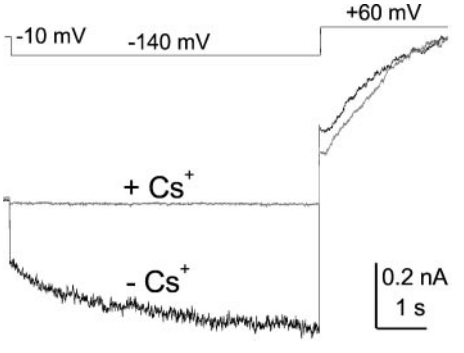

Figure 3. The effect of Cs^+. Top, Voltage pulse protocol. Bottom, Whole-cell current traces (superimposed) recorded from a flexor cell in the absence ($-Cs^+$) and in the presence ($+Cs^+$) of Cs^+ added to the bath to a final concentration of 10 mM. Note the contrast between the inward current block at -140 mV and the lack of any effect on the outward current at 60 mV (except of the initial phase, representing the different contributions of the "tail currents" resulting from the preceding pulse). Solutions: bath (c)/pipette (f).

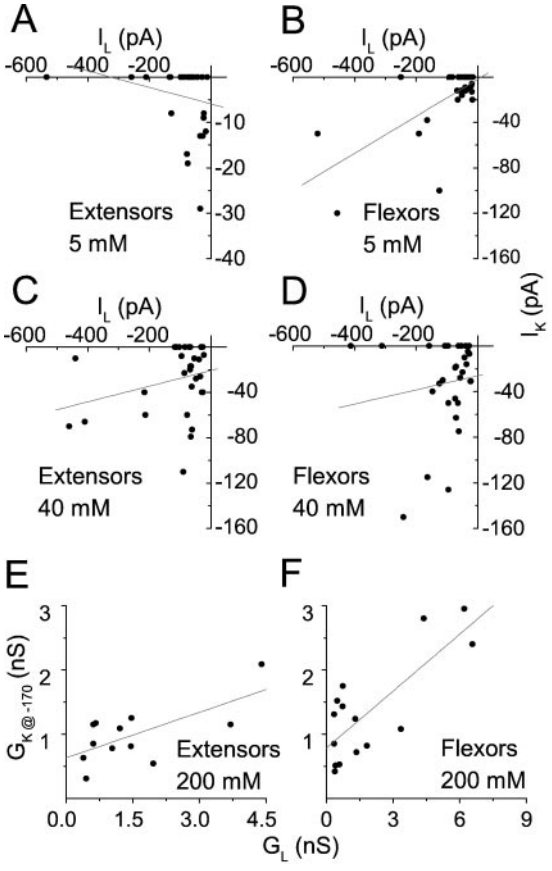

Figure 4. Correlation between leak and K_H channels. A through D, Correlation between currents. Symbols: paired values of I_K at steady state and I_L, determined in the same cells at −170 mV. The data were grouped separately according to the cell type (E, extensors; F, flexors) and the $[K^+]_O$ (as indicated; 30 cells in each category). Lines, Linear regressions to the data. E and F, Correlation between conductances. Symbols: G_L and $G_{K@-170}$ values, determined as described in "Materials and Methods" and paired by the cell of origin, as in A through D, were also grouped according to the cell type and $[K^+]_O$. Lines, Linear regressions to the data. The regression slopes and correlation coefficients were, respectively, as follows: in flexors at 5 mM, 0.16, 0.68, $P < 0.0001$ ($n = 30$); in extensors at 5 mM, −0.02, −0.24, $P < 0.2$ ($n = 30$); in extensors at 40 mM, 0.7, 0.28, $P < 0.14$ ($n = 30$); in flexors at 40 mM, 0.6, 0.14, $P < 0.47$ ($n = 30$); extensors at 200 mM, 0.24, 0.67, $P < 0.02$ ($n = 12$); and flexors at 200 mM, 0.30, 0.79, $P < 0.0005$ ($n = 15$). Solutions: b/f, b/h, c/f, or c/h.

preclude the calculation of the instantaneous conductance, G_L). We plotted G_K, the time-dependent chord conductance (see Eq. 1) of K_H channels at steady state, at −170 mV ($G_{K@-170}$) versus the conductance, in the same cell, of the leak pathways between −80 and −170 mV (G_L; Fig. 4, E and F; see "Materials and Methods" for details). At 200 mM, G_L was 2- to 4-fold larger than $G_{K@-170}$ in flexors ($n = 15$) and in extensors ($n = 12$). In these cells at 200 mM and in flexors at 5 mM ($n = 30$), both types of pathways were highly correlated, with R, the correlation coefficient, between 0.7 and 0.8. No correlation has been demonstrated, however, for these cells at 40 mM or for extensors at 5 mM K^+ ($n = 30$ in each group).

Single Channels

Hyperpolarization-activated unitary currents recorded from excised outside-out patches (Fig. 5A) appeared related to the whole-cell inward currents, as demonstrated by averaging 10 responses to a repeated −170-mV pulse (Fig. 5B). Moreover, when the external solution contained 37 mM Glu instead of Cl^-, and the calculated Nernst potential for Cl^- was +94 mV rather than +27 mV (E_K remained −29 mV), the pattern and the I-E_M relationships of the single-channel currents remained largely unaffected (e.g. compare Fig. 5, C and D with A and B). This indicates

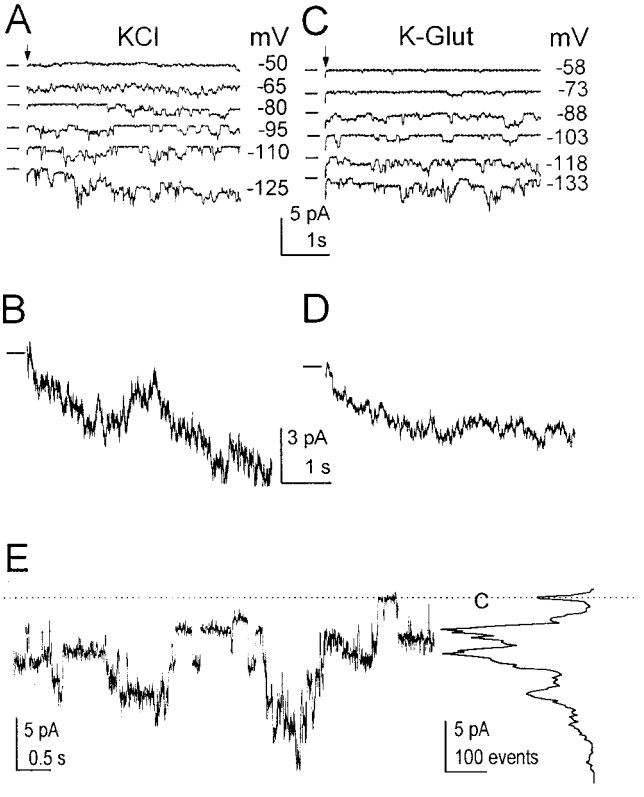

Figure 5. Single channels underlying the inward currents. A, Representative traces with unitary currents from an outside-out extensor patch bathed in solution (b) during steps (arrows) to the indicated membrane potentials, lasting 5 s. The inter-pulse-interval was 30 s. Solutions: (b)/(f). Note the downward deflections signifying channel opening. B, An average of 10 traces of current evoked by a repeated step to −170 mV in the patch of A. Note the gradually increasing inward current similar to the time-dependent whole-cell current in Figure 1A. The dash at the left indicates the closed-channel current. C and D, The same patch as in A, now bathed in solution (e). Note the similar pattern of activity (as in A and B). Pipette solution: (f). E, Single-channel activity at −110 mV (left), and a corresponding all-points amplitude histogram presented at the same current scale (right), to illustrate the complicated multilevel appearance of the unitary events. Dotted line and C, the closed-channels current level. Solutions: (c)/(f).

that these inward unitary currents were carried by influx of cations (K^+) rather than by efflux of anions. In the individual single channel records, we were unable to discern between the two channel types, the K_H and leak channels, which were presumably active simultaneously in the patches. The amplitudes of the unitary currents fluctuated widely, appearing to represent different size sublevels, rather than multiples of the same level (Fig. 5E). In addition, all of the 15 patches examined contained many channels. Therefore, detailed analysis of the unitary currents was abandoned.

K_H Channel Gating

The effects of 40 and 200 mM K^+ on I_K −170 mV, $I_{K@-170}$, were examined in the same whole cells. $I_{K@-170}$ increased with increased $[K^+]_O$ from −12 ± 5 to −131 ± 20 pA in seven extensors ($P < 0.01$) and from −27 ± 10 to −123 ± 33 pA in 10 flexors ($P < 0.05$). To test whether the increase of $[K^+]_O$ shifts the voltage dependence of the steady-state K_H channel gating to more positive potentials (as it does in the case of the outward-rectifying K_D channel; Moran et al., 1987; Blatt and Gradmann, 1997), we calculated the chord conductances (G_K) from the net time-dependent currents (Eq. 1) at all membrane potentials tested, and we fitted the averaged G_K-E_M relationships with the Boltzmann relationship (based on the simplest model of equilibrium between one closed and one open state, Eq. 3, Fig. 6). The mean fitted parameters are listed in Table I. $[K^+]_O$ did not seem to affect consistently the midactivation potential, $E_{1/2}$, even when $E_{1/2}$ was examined during concentration changes in the same cells (in three flexors and one extensor; not shown).

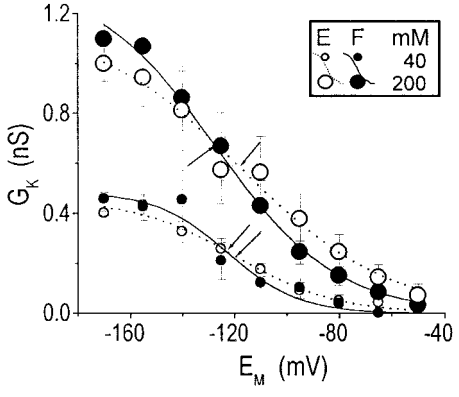

Figure 6. The effect of $[K^+]_O$ on K_H channel gating. G_K-E_M relationships (mean ± SE) of six extensors (E) and five flexors (F) at $[K^+]_O$ of 40 mM and from eight extensors and nine flexors at 200 mM. Lines are Boltzmann functions fitted to the averaged (G_K-E_M) data, with the best fit parameters listed in Table I (see "Materials and Methods" for details of averaging). Arrows indicate the $E_{1/2}$ values. Solutions as in Figure 1B.

Table I. *K_H channels gating parameters: effect of $[K^+]_O$*

Boltzmann best fit parameters (±SE) of the averaged "restored" G_K-E_M relationships of Figure 6 at two external K^+ concentrations. G_{max}, the asymptotic value of G_K at saturating potentials; $E_{1/2}$, the half-maximum-activation voltage; z, the effective number of gating charges (Eq. 3; see "Materials and Methods" for details).

Cell Type	Extensors		Flexors	
	(n = 6)	(n = 8)	(n = 5)	(n = 9)
	40 mM $[K^+]_O$	*200 mM* $[K^+]_O$	*40 mM* $[K^+]_O$	*200 mM* $[K^+]_O$
Parameter				
G_{max} (nS)	0.5 ± 0.0	1.2 ± 0.1	0.5 ± 0.1	1.3[a]
$E_{1/2}$ (mV)	−120 ± 4	−118 ± 7	−123 ± 5	−127 ± 1.1
z	1.3 ± 0.2	0.9 ± 0.1	1.9 ± 0.6	1.1 ± 0.1

[a] This G_{max} value (the mean of the individual G_{max} values of the G_K-E_M relationships prior to G_K averaging) was fixed during the fit. The other G_{max} values in the table were not different from the respective means of the individual G_{max}.

Effects of Extracellular pH

To test the effect of pH, we used 200 mM K^+ in the bath because these conditions yielded increased inward currents (Fig. 5). Lowering the external pH from 7.8 to 5.0 decreased I_K, and this effect appeared reversible (Fig. 7, A–D). The same was true for $G_{K@-170}$, but in contrast, it appeared that G_L was not affected by acidification (Fig. 7, E and F). In fact, each wash was accompanied by an increase in G_L. To resolve the effect of acidification on the steady-state K_H channel gating, we again fitted G_K-E_M relationships with the Boltzmann equation (Eq. 3; Fig. 8). In both extensors and flexors, acidification markedly decreased G_{max} (Table II). It is interesting that although restoring pH 7.8 also restored the G_{max}, $E_{1/2}$ in flexors became more negative than at $pH\ 7.8_I$ ($P < 0.02$; Fig. 8; Table II).

DISCUSSION

Identification of the *S. saman* K_H Channels

The dependence of single-channel activity on hyperpolarization (Fig. 5), the similarity of the time course of single channels recruitment to the time course of activation of whole-cell currents (Figs. 5B and 1A), and the insensitivity to drastic changes in the chloride Nernst potential (Fig. 5, A and C) all indicated that the single channels we observed included K_H channels. We were unable, however, to distinguish between K_H and leak channels. To our surprise, all the records from all the outside-out patches exhibited single-channel activity with an extremely wide range of unitary amplitudes. This is very different from the relatively uniform appearance of the inward-rectifying unitary currents via the K_H channels in patches from oocytes expressing KAT1-type channels (Zei and Aldrich, 1998), or AKT2/3 channels (Marten et al., 1999; Lacombe et al., 2000). Even the unitary currents of native, inward-

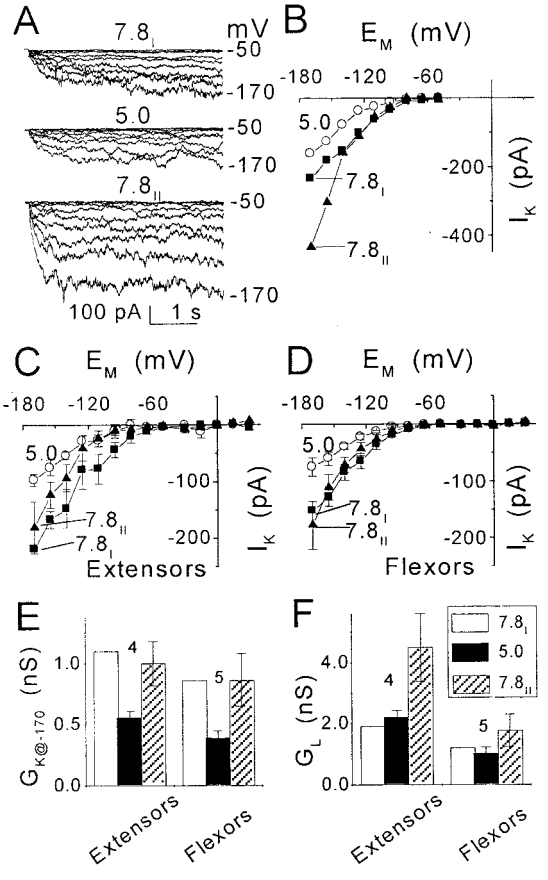

Figure 7. The effect of external pH on membrane conductance at $[K^+]_O$ of 200 mM (pipette solution: f). A, Inward currents in a flexor cell at the indicated pHs. Pulse protocol as in Figure 1A. Numbers at the right are the membrane potentials during the corresponding pulses. B, I-E_M relationships of the time-dependent current records in A during consecutive treatments at pH 7.8 (7.8_I), then at pH 5.0 and again at pH 7.8 (7.8_{II}). C and D, I-E_M relationships of the time-dependent currents (mean ± SE), compared at the two pHs in the same cells: four extensors and five flexors (see "Materials and Methods" for details of averaging). The mean (±SE) values of the extensors and flexors currents at pH 7.8 and −170 mV, used for the normalization and "restoration," were 219 ± 55 pA and 153 ± 29 pA, respectively. E and F, Comparison of conductances (mean ± SE, n), G_K at −170 mV ($G_{K@-170}$) and G_L (between −80 and −170 mV), in the extensors and flexors of C and D, at the different pHs. Prior to averaging, $G_{K@-170}$ at each pH was normalized to $G_{K@-170}$ at pH 7.8_I. The mean values used for normalization were 1.1 ± 0.2 nS in extensors and 0.8 ± 0.2 nS in flexors.

rectifying, plant channels described to date were much more uniform in appearance, such as those in outside-out patches from guard cell protoplasts with KAT1-type channels of broad bean (*Vicia faba*; Schroeder et al., 1987; Wu and Assmann, 1994; Ilan et al., 1996), or of potato (*Solanum tuberosum*; Dietrich et al., 1998), or even in an outside-out patch from a coleoptile vasculature protoplast, presumed to exhibit the activity of ZMKT2, an AKT2-like channel (Bauer et al., 2000). The same pattern of multilevel openings was also apparent in our records filtered at 500 Hz and sampled at 2 kHz (data not shown). Further work is required to resolve whether specific cytosolic components or intactness of the membrane are required for a more uniform amplitude of the unitary currents in *S. saman*, and/or whether this complicated pattern of activity reflects two populations of channels.

Another important difference between the guard cell and the pulvinar K_H channels revealed in this report is their opposite dependence on external acidification: In guard cells, channel activity was enhanced (Blatt, 1992; Ilan et al., 1996), whereas in pulvinar cells, channel activity was inhibited (Figs. 7 and 8). A similar difference was demonstrated between the guard cell KAT1-type channels (expressed in oocytes), which were activated by external acidification (Hoshi, 1995; Mueller-Roeber et al., 1995; Very et al., 1995; Hoth et al., 1997a) and the AKT2-type channels (also expressed in oocytes), which were inhibited by external acidification (Marten et al., 1999; Philippar et al., 1999; Lacombe et al., 2000). These contrasting findings suggest that the K_H channels revealed in electrophysiological experiments in guard cells and in pulvinar cells may have different molecular identity. In their pH dependency, the pulvinar K_H channels resemble the ZMK2-like channels in maize (*Zea mays*) coleoptiles (described in the first account of anin planta AKT2-like channel, Bauer et al., 2000 [published simultaneously with the completion of the present work]). Our recent cloning of two members of the AKT2 subfamily from whole pulvini (accession nos. AF099095 and AF145272) and the demonstration of their expression in the extensor and flexor tissues (Becker et al., 1998; M. Moshelion, D. Becker, and N. Moran, unpublished data) lend support to this notion.

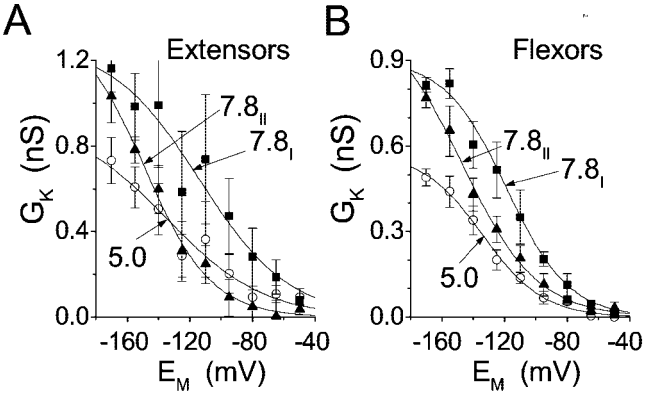

Figure 8. The effect of external pH on K_H channel gating. G_K-E_M relationships (mean ± SE) of A, four extensors, and B, five flexors at $[K^+]_O$ of 200 mM at the indicated pHs. Lines are Boltzmann functions fitted to the averaged (G_K- E_M) data, with the best fit parameters listed in Table II (see "Materials and Methods" for details of averaging). Arrows indicate $E_{1/2}$ values. Note the progressive shift of $E_{1/2}$ to more negative values. Solutions: bath: (c) or (d)/pipette: (f).

Table II. *K_H channels gating parameters: effect of external pH*

Reversal potentials (E_{rev}) used to calculate G_K, and Boltzmann best fit parameters (±SE) to the averaged "restored" G_K-E_M relationships of Figure 7 at the different pHs. The subscripts I and II denote the first and the last treatments with pH 7.8. The other definitions are as in Table I (see "Materials and Methods" for details).

Cell Type	Extensors (4)			Flexors (5)		
	pH 7.8_I	pH 5.0	pH 7.8_{II}	pH 7.8_I	pH 5.0	pH 7.8_{II}
Parameter						
E_{rev} (mV)	6.4 ± 0.6	5.5 ± 1.8	6.8 ± 1.5	7.3 ± 1.0	8.8 ± 1.2	6.7 ± 1.9
G_{max} (nS)	1.3 ± 0.2	0.9[a]	1.4 ± 0.2	0.9 ± 0.1	0.6 ± 0.0	1.1 ± 0.1
$E_{1/2}$ (mV)	−117 ± 13	−134 ± 3	−149 ± 7	−119 ± 4	−134 ± 4	−147 ± 6
z	0.9 ± 0.2	0.8 ± 0.1	1.2 ± 0.2	1.3 ± 0.2	1.3 ± 0.1	1.1 ± 0.1

[a] This G_{max} value (the mean of the individual G_{max} values of the G_K-E_M relationships obtained prior to G_K averaging) was fixed during the fit. The other G_{max} values in the table were not different from the respective means of the individual G_{max}.

The Instantaneous and Time-Dependent Currents: A Single Interconverting Channel or Two Separate Conduits?

Recent reports on the inward voltage-dependent K^+ currents via AKT2 channels expressed in oocytes, as well as on the ZMK2-like channel of maize, attributed the instantaneous and the time-dependent currents to the same channel (Marten et al., 1999; Philippar et al., 1999; Lacombe et al., 2000). The report on ZMK2-like channels in maize cells followed suit, adopting a similar approach (Bauer et al., 2000). Because of the danger inherent to heterologous expression systems of evoking endogenous activity, we decided to reexamine the issue in the *S. saman* model.

Biophysical and pharmacological approaches support the notion that the leak pathway contains a K^+ conduit, similar to the K_H channel. In our experiments, the reversal potential of the instantaneous currents, E_L, was significantly lower than the calculated reversal potential of the "seal leak" (i.e. the liquid junction potential of 0 mV between the pipette and the bath solutions; see Fig. 2). Only an increased membrane conductance to one (or both) of the cations K^+ and Mg^{2+}, with negative equilibrium potentials, would be capable of shifting E_L away from 0 mV at $[K^+]_O$ of 5 and 40 mM. While G_L was of the same order of magnitude as the seal conductance (0.1–1 S), perfectly K^+-selective channels would have to constitute well over one-half of the total leak conductance to shift E_L from 0 to −17 mV (calculated based on the equivalent circuit model [Hille, 1992]) and E_K of −30 mV. Indeed, the leak pathway was largely blocked by Cs^+ (Fig. 3).

Does only one interconverting molecule underlie both K^+ conductances? Two lines of evidence indicate that leak channels (I_L and G_L) and K_H channels (I_K and G_K) might be separate. G_L and G_K were not correlated in three cases: in extensors and flexors at 40 mM and in extensors at 5 mM (Fig. 4). G_K decreased significantly with acidification, whereas G_L did not (Fig. 7, E and F). However, this lack of G_L susceptibility to pH could be only apparent; for example, it could be due to an increasing fraction of nonspecific leak resulting from the worsening of pipette seal with each bath wash (inexplicably, this was pronounced more in flexors than in extensors).

An argument in favor of the single-molecule hypothesis in the case of *S. saman* is the remarkable increase of both I_K and I_L with $[K^+]_O$ (Fig. 1 and text). However, such a correlation is expected for K channels.

Another piece of evidence suggesting that I_L and I_K, or G_K and G_L, represent the same channel is the correlation between the two types of pathways in cells grouped by type and concentration (in three out of six cases examined: in flexors at 5 mM external $[K^+]$, and in extensors and flexors at 200 mM; Fig. 4). However, this correlation may simply reflect the activity of a regulatory mechanism common to these pathways, even if they are distinct.

Finally, the "same channel" notion is favored by a similarity in the pharmacological effects: Not only were I_L and I_K blocked similarly by Cs^+, but they were also (at least in flexors) similarly insensitive to TEA, a rather uncommon behavior of K channels. Taken together, all of these results suggest that an important component of the leak in *S. saman* motor cells may consist of modified, voltage-independent, K_H channels.

Physiological Relevance: Both K_H Channels and Leak Pathways Are Probably Important for K^+ Influx

K^+ influx channels are presumed to play the same roles in the swelling of cells in the flexor and extensor parts of the pulvinus, although they are regulated by different signaling cascades (Kim et al., 1993, 1996; Suh et al., 2000). In our experiments with isolated protoplasts in a whole-cell configuration, no significant differences between inward currents have been found between both cell types, and therefore we have not separated them in our discussion.

We base our estimate of the transmembranal K^+ flux in the pulvini on the osmolarity differences be-

tween the swollen and contracted states in flexors and extensors in situ of approximately 350 and approximately 400 mOsm, respectively (Gorton, 1987). Attributing it all in roughly equal parts to K^+ and Cl^- (Satter and Galston, 1981) means that $[K^+]$ fluctuations in the cells are within about 200 mM. Based on an average diameter of a motor cell protoplast of 30 μm (Moran et al., 1988) and extrapolating to an intact pulvinus, this amounts to roughly 3 pM K^+ exchanged across the cellular membrane during pulvinar movement.

Can K_H Channels Alone Mediate All of the K^+ Uptake Necessary for the Swelling of S. saman Motor Cells?

To calculate this, we used the following values for the parameters of Equation 1 ("Materials and Methods"): We assumed an E_M of -150 mV (a swelling stimulus to a flexor cell wounded by a membrane-penetrating microelectrode hyperpolarized the cell to -60 mV [Racusen and Satter, 1975]; hence, in an intact motor cell, a hyperpolarization to -150 mV is a realistic estimate). We assumed an E_K of -35 mV based on an internal K^+ activity of 80 mM (Gorton and Satter, 1984) and an average external K^+ activity of 20 mM (the apoplastic in situ activity of K^+ measured in the swelling extensor of the *S. saman* pulvinus changed between 70 and 15 mM and in the swelling flexor from approximately 25 to approximately 10 mM [Lowen and Satter, 1989]). Based on the two former assumptions, average driving force for K^+ influx was -115 mV. With a cell conductance due to K_H channels alone (G_K) of 0.4 nS (based on Fig. 6), the predicted amount of K^+ entering the *S. saman* motor cell during about 1 h of swelling would be only 1.7 pM. Even this is probably a "higher end" estimate based on data from channels with the larger I_K currents. Thus, influx via K_H channels alone seems to be insufficient to account for the estimated changes in K^+ within 1 h or less, during which a significant movement can occur. However, the parallel conduit, leak (G_L), appears to offer similarly K^+-specific, but usually much larger conductance than do K_H channels (Fig. 4). We conclude, therefore, that unless K_H channel activity in the motor cells in situ is considerably higher than in isolated protoplasts (the relatively higher K_H channel activity in excised patches suggests that this is possible; data not shown), the leak channels are indispensable, along with the K_H channels, for the influx of K^+ into the swelling pulvinar cells.

pH Effect

The current paradigm led us to expect that the H^+-ATPase-powered K^+ uptake in the pulvinar motor cells occurs via the inward-rectifying K channels, functioning as do their counterparts in guard cells. Resembling guard cells, the swelling of the pulvinar motor cells coincided with quite significant external acidification: The apoplastic pH in *S. saman* pulvini decreased from 5.4 to 4.8 in flexors and from 7.1 to $\leq$6.2 in extensors during the first 20 min of the swelling phase (Lee and Satter, 1989). The unexpected finding that opposite to the behavior of the guard cell K_H channels, the *S. saman* K_H channels are considerably less active at an external pH 5.0 than at pH 7.8, means—at least in the case of flexors—that K^+ influx via K_H channels in the swelling pulvinar cells is even smaller than that calculated above. Whether or not leak channels are unaffected by acidification (Fig. 7), they are likely to play an important role in K^+ uptake.

K_H Channels in Guard Cells and Pulvinar Cells: The Two Models Compared

In rather similar conditions, i.e., at pH close to 8 and $[K^+]_O$ of 11 mM, G_L of guard cells was similar to that in pulvini; normalized to surface area, they were both about approximately 40 μS cm^{-2}. In contrast to the similarity in G_L, the two cell types were greatly dissimilar in their G_K values. In guard cells, G_K was about 100-fold larger than G_L (normalized to surface area, G_K was 4.5 mS cm^{-2}; Ilan et al., 1996). In pulvini, G_K was at least 2- to 4-fold smaller than G_L (Fig. 4, E and F). The large G_K in guard cells appears to stem from the activity of KAT1 and KAT2 twin channels (Pilot et al., 2001), with an unknown contribution of other channels (Szyroki et al., 2001). In pulvinar cells, unless similar channels are revealed in different experimental conditions, the much smaller G_K may reflect the activity of AKT2-like channels alone. The inhibition of these pulvinar K_H channels by protons (as well as by Cs^+, but not by TEA) provides an important characteristic trait that will be used in the quest for their molecular identification.

In conclusion, the guard cell paradigm of swelling needs to be modified for the pulvinar motor cells to include the inhibitory effect of pH on K_H channels, and the more than probable participation of the leak channels as K^+ influx conduits.

MATERIALS AND METHODS

Plant Material

Samanea saman Merr. trees (referred to also as *Pithecellobium saman* Benth. [Little and Wadsworth, 1964], or as "saman," one of its common names throughout Latin America, or as "Samanea," in earlier physiological literature) were grown in a greenhouse or in a growth chamber under 16-h-light/8-h-dark schedule. The day illumination in the greenhouse (supplemented by Fluora lamps, Osram, Munich) was 300 to 700 μmol m^{-2} s^{-1}, the temperature ranged between 18°C and 50°C, and the humidity was 60% to 90%. In the growth chamber the illumination was 50–100 μmol m^{-2} s^{-1}, the temperature was 28°C to 30°C, and the

humidity was 75% to 85%. Data from plants grown in both environments were pooled together.

Preparation of Protoplasts

Terminal secondary pulvini were harvested from the second and third mature leaves, counting from the top, within 3 h before or after dawn (in the growth chamber or the greenhouse, respectively). Protoplasts were isolated separately from the extensor and flexor regions of the pulvinus about 5 h following the harvest. The isolation procedure (Moran et al., 1988; Moran, 1996) was modified as follows: The freshly chopped tissue pieces were rinsed on a 20-μm mesh filter with solution containing 0.1% (w/v) polyvinylpyrrolidone to neutralize the possible effects of endogenous phenolics, the osmolarity of the enzyme solution was increased with sorbitol to 780 mOsm, and the osmolarity of protoplast incubation solution was maintained at 720 mOsm. The isolated protoplasts were kept on ice for up to 10 h under constant low-level illumination (approximately 2 μmol m^{-2} s^{-1}) until use.

Patch-Clamp Procedure

The experiments were conducted at room temperatures between 23°C and 25°C, with ≤1°C variation during a single experiment. Application of the patch-clamp methodology (Hamill et al., 1981) to *S. saman* protoplast was described by Satter and Moran (1988). Patch-clamp pipettes were prepared from borosilicate glass (catalog no. BF150-86-10, Sutter Instrument Company, Novato, CA) by two-stage pull and fire polishing, yielding tips with resistances between 5 and 10 MΩ (measured with an internal pipette solution and a 5 mM K^+ external solution in the bath, solution a). The protoplasts were added into an approximately 300-μL chamber, allowed to settle on the glass bottom for 10 to 15 min, and flushed with 4 mL of solution a, used to promote protoplast-pipette sealing. The seal resistance was between 1 and 10 GΩ. After attaining a "whole-cell" configuration and a few test records (approximately 10 min), the chamber was perfused with a 40 or 200 mM K^+-external solution (solution b or c) aimed at eliciting inward current. The bridge of the reference electrode was filled with the same solution as the external recording solution chosen for prolonged recording in the particular experiment. All experiments were performed in a voltage-clamp mode (with an Axopatch B-1 amplifier, Axon Instruments, Foster City, CA) and were under computer control using a software-hardware system from Axon Instruments (pClamp program package software, version 5.5.1, and the TL1- TM-100 Labmaster A/D and D/A peripherals). Membrane potential was varied according to preprogrammed pulse protocols (detailed below).

The holding potential, restored between pairs of pulses, depended on the external solutions used: It was −80 mV with 5 mM K^+ outside, −40 or −30 mV with 40 mM K^+ outside, and between −30 and 0 mV with 200 mM K^+ outside. Two pulse sequences were used during the experiments. To monitor the voltage and time dependence of the inward-rectifying K^+ channels (the K_H channels), a series of increasingly hyperpolarizing single square pulses was applied at 25-s intervals between start of pulses (Fig. 1A, top). Each of the 8-s-long pulses, ranging between −50 and −155 or −170 mV, at −15-mV steps, were followed by a depolarization to +50 mV to enhance the deactivation of hyperpolarization-activated channels. To identify the selectivity of the channels, E_{rev} was determined by a "tail current" method consisting of a series of paired pulses (a constant main prepulse and a variable test pulse, denoted c and d, respectively, in Fig. 9, top), applied at 25-s intervals. The main prepulse, aimed to open the hyperpolarization-activated channels, was always the same for a given series (4 s, −170 mV), whereas the test pulses ranged from −60 to 15 mV with 40 mM K^+ in the bath, or from −30 to 15 mV with 200 mV K^+ (usually aimed at the vicinity of the presumed reversal potential). To obtain the "leak" current (reflecting the conductance of channels open at the holding potentials, as well as nonspecific conductances), each main prepulse was preceded by a brief pulse of the same amplitude as the corresponding test pulse, before any channel has had the chance to open (Fig. 9a). The currents were filtered via a 4-pole Bessel filter of the patch-clamp amplifier, with a −3dB point of 50 Hz, sampled at a frequency of 250 Hz.

Single-channel currents were recorded in an "outside-out" configuration, similarly filtered at 50 Hz and sampled at 250 Hz (Fig. 5, A–D), or filtered at 500 Hz and sampled at 2 kHz (Fig. 5E). The record of Figure 5E was subsequently filtered for display (software Gauss filter) at 200 Hz.

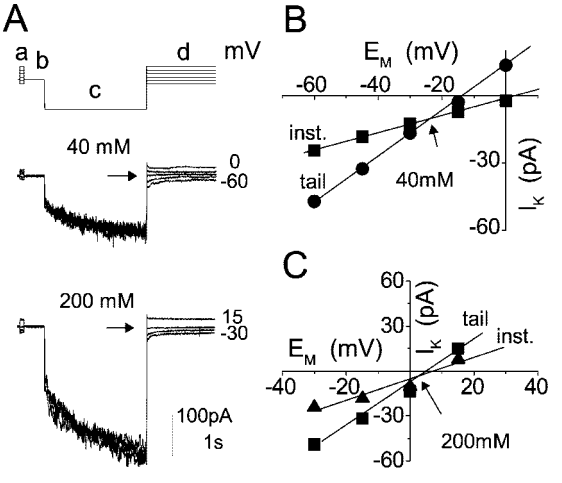

Figure 9. Determination of reversal potentials by the "tail current" method. A, Pulse protocol (top) elicited inward currents from a flexor cell at $[K^+]_O$ of 40 and 200 mM (superimposed records, middle and bottom). a and d, Varying pre- and test- pulses; b, holding potential; c, the main prepulse. Numbers at the right are the membrane potentials during the corresponding test pulses. Arrows mark the level of current at the reversal potential. Solutions used: bath, b or c with pipette f. B and C, I-E_M relationships of the instantaneous (inst.) currents in A, sampled during a (▲) and the zero-time tail current sampled at the onset of d (■), at the indicated $[K^+]_O$. Arrows mark the reversal potential of the time-dependent current, E_{rev}, −24 mV at 40 mM and +5 mV at 200 mM.

Corrections

On-Line

When recording in the whole-cell configuration, the error in the voltage clamping of the whole-cell membrane, largely due to the series resistance (Rs) of the patch pipette was compensated at approximately 80% by analog circuitry of the amplifier. Mean Rs was 35 ± 1 MΩ (±SE, n = 30).

On-Line: Holding Current Subtraction

Because at $[K^+]_O$ of 200 mM the amplitude of the instantaneous currents was frequently larger than that of the time-dependent currents, to avoid amplifier saturation (while preserving the large gain), the holding current at this concentration was usually sampled at the onset of each experiment and was automatically subtracted from all of the subsequent records (using the "zero-reset" capability of the patch-clamp amplifier). Therefore, at 200 mM K^+, the I-E_M curves of the instantaneous currents are expected to cross the abscissa at the holding potentials (between −30 and 0 mV; Fig. 1C, bottom), rather than at their true reversal potentials.

Off-Line

The liquid junction potential between the recording solutions with Cl^- as the main anion was below 1 mV (calculated using ion mobilities and activities, Robinson and Stokes, 1965), and therefore no correction was performed. When Glu replaced Cl^- in the external solution, i.e., in solution e, the liquid junction potential between solution e and g was measured directly (separately from the experiments), using bridges with 3 M KCl/agar (Neher, 1992) and its value of 3 mV was added to the nominal value of membrane potential.

Analysis

Whole-Cell Currents

The appropriate values of current from the two types of pulse sequences were used to plot the current-voltage (I-E_M) curves: the instantaneous currents recorded immediately after the voltage jump, and the steady-state total current recorded just before the end of the pulse.

I_K Averaging

To diminish the noise originating from the biological variation among cells, the values of I_K were averaged only after normalization to each cell's own I_K at −170 mV. For presentation, the averaged normalized values (and their errors) were "restored" by multiplying them by the original mean values of these currents at −170 mV (as in Ilan et al., 1994).

E_{rev} and G_K

The determination of the E_{rev} from the I-E_Ms of the instantaneous currents in the "tail current method," as well as the determination of the membrane chord conductance for K^+, G_K from the time-dependent currents, rest on the following relationship (Hodgkin and Huxley, 1952):

$$I_K = G_K(E_M - E_{rev}) \quad (1)$$

where I_K is the K^+ current at steady state and E_M is the membrane potential. E_{rev} was compared with the calculated equilibrium potential (Nernst potential) of each permeant ion:

$$F_x = RT/z'F\ ln([X]_{in}/[X]_{out}) \quad (2)$$

where E_x is the equilibrium potential of the X ion, R is the universal gas constant, T is the absolute temperature, z′ is the valence of the X ion, and [X] is its activity. When possible, E_{rev} was determined for each cell separately. However, for the calculation of G_K in the groups of 40 and 200mMK^+, themeanE_{rev} values of some cells were used for the other cells from their own group. G_K was fitted with the Boltzmann relationship to describe the voltage dependence of channel gating (Ehrensteinetal.,1970):

$$G_K = G_{max}/1 + e^{Z\,(E_M - E_{1/2})\,F/RT} \quad (3)$$

where G_{max} is the maximum conductance of K_H channel in the whole cell membrane, $E_{1/2}$ is the half-maximum-activation membrane potential, and z is the effective number of gating charges. G_{max} reflects the single-channel conductance, γ_S, times the channel "availability" (the maximum mean number of open channels in the patch), consisting, in turn, of the product of the channel protein abundance in the membrane, N, and their voltage-independent opening probability, f_O (Ilan et al., 1996):

$$G_{max} = N \times f_O \cdot \gamma_S \quad (4)$$

G_K Averaging

To minimize the noise, prior to averaging, the G_K-E_M curves of each cell were first fitted with a Boltzmann function (Eq. 3) and then each cell's own G_{max} was used for normalization (in Fig. 7, the G_{max} of the first treatment, pH 7.8, was used). Then, the G-E_M curves were averaged separately, in groups according to cell type and treatment, and finally they were "restored" to their original range of values by multiplying by the corresponding mean of the G_{max} values used for normalization, and fitted with the Boltzmann curve. The final best fit G_{max} values listed in Tables I and II did not differ from the particular values used for averaging and "restoring."

G_L, the instantaneous membrane conductance, was determined from two values of current at −80 and −170 mV, based on the relative linearity of its I-E_M relationship at this range (as in Fig. 1C).

Statistics

Means are presented with their standard errors (±SE, unless otherwise indicated), with n as the number of cells averaged. Differences between means were deemed signif-

icant if, using a two-sided Student t test, $P < 0.05$. Higher levels of significance are indicated in the text.

Solutions

The external solution contained D-sorbitol, adjusting the osmolarity from 700 to 730 mOsm, and in addition, one of the following combinations: (a) 5 mM KOH, 1 mM $CaCl_2$, and 9.5 mM MES [2-(*N*-morpholino)-ethanesulfonic acid], pH 6.0; (b) 1 mM KOH, 39 mM KCl, 0.3 mM $CaCl_2$, and 10 mM HEPES [4-(2-hydroxyethyl)-1-piperazineethanesulfonic acid], pH 7.8; (c) 2 mM KOH, 198 mM KCl, 0.3 mM $CaCl_2$, 10 mM HEPES, and 6 mM *N*-methyl-D-glucamine, pH 7.8; (d) 2 mM KOH, 198 mM KCl, 0.3 mM $CaCl_2$, and 16 mM MES, pH 5.0; and (e) 1 mM KOH, 2 mM KCl, 37 mM K-Glu, 0.3 mM $CaCl_2$, and 10 mM HEPES, pH 7.8. The internal solution contained 125 mM KCl, 1 mM $MgCl_2$, 20 mM HEPES, and 8 mM *N*-methyl-D-glucamine, at pH 7.8, D-sorbitol, adjusting the osmolarity to 750 mOsm, and in addition: (f) 2 mM ATP-K_2 and 2 mM 1,2-bis(o-aminophenoxy)ethane-N;N;N;N-tetraacetic acid (BAPTA)-K_4, or (g) 4 mM ATP-K_2 and 2 mM BAPTA-K_4, or (h) 4 mM ATP-K_2 and 6 mM BAPTA-K_4.

Based on the assumption that the internal solution was contaminated with <10 μM total Ca^{2+}, the calculated activity of free Ca^{2+} in all the internal solutions was approximately 10 to 30 nM. The calculated free Mg^{2+} activity was approximately 200 μM, and the activity of free ATP was approximately 20 to 30 μM. These calculations were performed using the "Geochem" program (Parker et al., 1995) with the following $-$log of absolute stability constants of ATP complexes at 21°C: ATP-Ca^{2+}, 4.0, 1.8; ATP-Mg^{2+}, 4.3 and 2.7; ATP-H^+, 7.1, 4.2, 1.0, and 1.0; and ATP-K^+, 0.9 (Fabiato, 1988), and $-$log of apparent stability constant of BAPTA-Ca^{2+}: 6.7 (at pH 7, ionic strength 0.1 M, and in the presence of 1 mM Mg, Pehtig et al., 1989).

BABTA-K_4 was from Molecular Probes (Eugene, OR) and other chemicals were from Sigma (St. Louis) or MERCK (Rahway, NJ) and were of analytical grade.

ACKNOWLEDGMENTS

The authors are grateful to Prof. Rainer Hedrich and Dr. Dirk Becker for helpful suggestions.

Received April 9, 2001; returned for revision May 25, 2001; accepted July 24, 2001.

LITERATURE CITED

Assmann SM, Simoncini L, Schroeder JI (1985) Blue light activates electrogenic ion pumping in guard cell protoplasts of *Vicia faba*. Nature **318:** 285–287

Baizabal-Aguirre VM, Clemens S, Uozumi N, Schroeder JI (1999) Suppression of inward-rectifying K^+ channels KAT1 and AKT2 by dominant negative point mutations in the KAT1 alpha-subunit. J Membr Biol **167:** 119–125

Bauer CS, Hoth S, Haga K, Philippar K, Aoki N, Hedrich R (2000) Differential expression and regulation of K^+ channels in the maize coleoptile: molecular and biophysical analysis of cells isolated from cortex and vasculature. Plant J **24:** 139–145

Becker D, Dreyer I, Hoth S, Reid JD, Busch H, Lehnen M, Palme K, Hedrich R (1996) Changes in voltage activation, Cs^+ sensitivity, and ion permeability in H5 mutants of the plant K^+ channel KAT1. Proc Natl Acad Sci USA **93:** 8123–8128

Becker D, Moshelion M, Czempinski K, Moran N, Hedrich R (1998) Molecular and biophysical analysis of ion channels in motor cells. *In* M Tester, C Morris, J Davies, eds, 11th International Workshop on Plant Membrane Biology. Springer Verlag, Cambridge, UK, p 118

Blatt MR (1985) Extracellular potassium activity in attached leaves and its relation to stomatal function. J Exp Bot **36:** 240–251

Blatt MR (1992) K^+ channels of stomatal guard cells: characteristics of the inward rectifier and its control by pH. J Gen Physiol **99:** 615–644

Blatt MR, Gradmann D (1997) K^+-sensitive gating of the K^+ outward rectifier in *Vicia* guard cells. J Membr Bio **158:** 241–256

Bowling DJF (1987) Measurements of the apoplastic activity of K^+ and Cl^- in the leaf epidermis of *Commelina communis* in relation to stomatal activity. J Exp Bot **38:** 1351–1355

Bruggemann L, Dietrich P, Becker D, Dreyer I, Palme K, Hedrich R (1999) Channel-mediated high-affinity K^+ uptake into guard cells from *Arabidopsis*. Proc Natl Acad Sci USA **96:** 3298–3302

Cao Y, Crawford NM, Schroeder JI (1995) Amino terminus and the first four membrane-spanning segments of the *Arabidopsis* K^+ channel KAT1 confer inward-rectification property of plant-animal chimeric channels. J Biol Chem **270:** 17697–17701

Czempinski K, Gaedeke N, Zimmermann S, Muller Rober B (1999) Molecular mechanisms and regulation of plant ion channels. J Exp Bot **50:** 955–966

Dietrich P, Dreyer I, Wiesner P, Hedrich R (1998) Cation sensitivity and kinetics of guard-cell potassium channels differ among species. Planta **205:** 277–287

Dreyer I, Horeau C, Lemaillet G, Zimmermann S, Bush DR, Rodriguez-Navarro A, Schachtman DP, Spalding EP, Sentenac H, Gaber RF (1999) Identification and characterization of plant transporters using heterologous expression systems. J Exp Bot **50:** 1073–1087

Edwards MC, Smith GN, Bowling DJF (1988) Guard cells extrude protons prior to stomatal opening: a study using fluorescence microscopy and pH microelectrode. J Exp Bot **39:** 1541–1547

Ehrenstein G, Lecar H, Nossal R (1970) The nature of the negative resistance in bimolecular lipid membranes containing excitability inducing material. J Gen Physiol **55:** 119–133

Erath F, Ruge WA, Mayer W-E, Hampp R (1988) Isolation of functional extensor and flexor protoplasts from *Phaseolus coccineus* L. pulvivni: potassium-induced swelling. Planta **173:** 447–452

Fabiato A (1988) Computer programs for calculating total from specified free or free from specified total ionic

concentrations in aqueous solutions containing multiple metals and ligands. Methods Enzymol **157:** 378–417

Fairley-Grenot KA, Assmann SM (1992a) Permeation of Ca^{2+} through K^+ channels in the plasma membrane of *Vicia faba* guard cells. J Membr Biol **128:** 103–113

Fairley-Grenot KA, Assmann SM (1992b) Whole-cell K^+ current across the plasma membrane of guard cells from a grass: *Zea mays*. Planta **186:** 282–293

Fairley-Grenot KA, Assmann SM (1993) Comparison of K^+ channel activation and deactivation in guard cells from a cotyledon (*Vicia faba* L.) and a graminaceous monocotyledon (*Zea Mays*). Planta **189:** 410–419

Freudling C, Starrach N, Flach D, Gradmann D, Mayer W-E (1988) Cell walls as reservoirs of potassium ions for reversible volume changes of pulvinar motor cells during rhythmic leaf movements. Planta **175:** 193–203

Gorton HL (1987) Water relations in pulvini from *Samanea saman*: I. Intact pulvini. Plant Physiol **83:** 945–950

Gorton HL, Satter RL (1984) Extensor and flexor protoplasts from *Samanea* pulvini: I. Isolation and initial characterization. Plant Physiol **76:** 680–684

Grabov A, Blatt MR (1999) A steep dependence of inward-rectifying potassium channels on cytosolic free calcium concentration increase evoked by hyperpolarization in guard cells. Plant Physiol **119:** 277–287

Hamill OP, Marty A, Neher E, Sakman B, Sigworth FJ (1981) Improved patch-clamp techniques for high-resolution current recording from cells and cell-free membrane patches. Pflueg Arch **391:** 85–100

Hille B (1992) Classical biophysics of the Squid Giant Axon. *In* Ionic Channels of Excitable Membranes, Ed 2. Sinauer Associates, Sunderland, MA, pp 337–361

Hodgkin AL, Huxley AF (1952) A quantitative description of membrane current and its application to conduction and excitation in nerve. J Physiol **117:** 500–544

Hoshi T (1995) Regulation of voltage dependence of the KAT1 channel by intracellular factors. J Gen Physiol **105:** 309–328

Hoth S, Dreyer I, Dietrich P, Becker D, Mueller Roeber B, Hedrich R (1997a) Molecular basis of plant-specific acid activation of K^+ uptake channels. Proc Natl Acad Sci USA **94:** 4806–4810

Hoth S, Dreyer I, Hedrich R (1997b) Mutational analysis of functional domains within plant K^+ uptake channels. J Exp Bot **48:** 415–420

Humble GD, Rashke K (1971) Stomatal opening quantitatively related to potassium transport: evidence from electron probe analysis. Plant Physiol **48:** 447–453

Ichida AM, Pei ZM, Baizabal Aguirre VM, Turner KJ, Schroeder JI (1997) Expression of a Cs^+-resistant guard cell K^+ channel confers Cs^+-resistant, light-induced stomatal opening in transgenic *Arabidopsis*. Plant Cell **9:** 1843–1857

Iglesias A, Satter RL (1983) H^+ fluxes in excised *Samanea* motor tissue: I. Promotion by light. Plant Physiol **72:** 564–569

Ilan N, Schwartz A, Moran N (1994) External pH effects on the depolarization-activated K channels in guard cell protoplasts of *Vicia faba*. J Gen Physiol **103:** 807–831

Ilan N, Schwartz A, Moran N (1996) External protons enhance the activity of the hyperpolarization-activated K channels in guard cell protoplast of *Vicia faba*. J Membr Biol **154:** 169–181

Kelly WB (1995) Effects of cytosolic calcium and limited, possibly dual, effects of G protein modulators on guard cell inward potassium channels. Plant J **8:** 479–489

Kim HY, Cote GG, Crain RC (1992) Effects of light on the membrane potential of protoplasts from *Samanea saman* pulvini: involvement of the H^+-ATPase and K^+ channels. Plant Physiol **99:** 1532–1539

Kim HY, Cote GG, Crain RC (1993) Potassium channels in *Samanea saman* protoplasts controlled by phytochrome and the biological clock. Science **260:** 960–962

Kim HY, Cote GG, Crain RC (1996) Inositol 1,4,5-trisphosphate may mediate regulation of K^+ channels by light and darkness in *Samanea saman* motor cells. Planta **198:** 279–289

Lacombe B, Pilot G, Michard E, Gaymard F, Sentenac H, Thibaud JB (2000) A shaker-like K^+ channel with weak rectification is expressed in both source and sink phloem tissues of *Arabidopsis*. Plant Cell **12:** 837–851

Lee Y, Satter RL (1989) Effects of white, blue, red light and darkness on pH of the apoplast in the *Samanea* pulvinus. Planta **178:** 31–40

Lemtiri-Chlieh F, MacRobbie EA (1994) Role of calcium in the modulation of *Vicia* guard cell potassium channels by abscisic acid: a patch-clamp study. J Membr Biol **137:** 99–107

Li JX, Lee YRJ, Assmann SM (1998) Guard cells possess a calcium-dependent protein kinase that phosphorylates the KAT1 potassium channel. Plant Physiol **116:** 785–795

Little ERJ, Wadsworth FH (1964) Common Trees of Puerto Rico and the Virgin Islands. U.S. Department of Agriculture, Washington, DC

Lowen CZ, Satter RL (1989) Light-promoted changes in apoplastic K^+ activity in the *Samanea saman* pulvinus, monitored with liquid membrane microelectrodes. Planta **179:** 421–427

Marten I, Hoth S, Deeken R, Ache P, Ketchum KA, Hoshi T, Hedrich R (1999) AKT3, a phloem-localized K^+ channel, is blocked by protons. Proc Natl Acad Sci USA **96:** 7581–7586

Moran N (1990) The role of ion channels in osmotic volume changes in *Samanea* motor cells analyzed by patch-clamp methods. *In* RL Satter, HL Gorton, TC Vogelmann, eds, The Pulvinus: Motor Organ for Leaf Movement 3. American Society of Plant Physiologists, Rockville, MD, pp 142–158

Moran N (1996) Membrane-delimited phosphorylation enables the activation of the outward-rectifying K channels in a plant cell. Plant Physiol **111:** 1281–1292

Moran N, Ehrenstein G, Iwasa K, Mischke C, Bare C, Satter RL (1988) Potassium channels in motor cells of *Samanea saman*: a patch-clamp study. Plant Physiol **88:** 643–648

Moran N, Iwasa K, Ehrenstein G, Mischke C, Bare C, Satter RL (1987) Effects of external K^+ on K channels in *Samanea* protoplasts. Plant Physiol **83:** 112S

Mueller-Roeber B, Ellenberg J, Provart N, Willmitzer L, Busch H, Becker D, Dietrich P, Hoth S, Hedrich R (1995) Cloning and electrophysiological analysis of KST1, an inward rectifying K^+ channel expressed in potato guard cells. EMBO J **14:** 2409–2416

Nakamura RL, McKendree WL-J, Hirsch RE, Sedbrook JC, Gaber RF, Sussman MR (1995) Expression of an *Arabidopsis* potassium channel gene in guard cells. Plant Physiol **109:** 371–374

Neher E (1992) Correction for liquid junction potentials in patch clamp experiments. Methods Enzymol **207:** 123–131

Parker DR, Norvell WA, Chaney RL (1995) GEOCHEM-PC: a chemical speciation program for IBM and compatible personal computers. *In* RH Loeppert, AP Schwab, S Goldberg, eds, Chemical Equilibrium and Reaction Models 42. SSSA Special Publication, Madison, WI, pp 253–269

Pehtig R, Kuhn M, Payne R, Adler E, Chen T-H, Jaffe LF (1989) On the dissociation constants of BAPTA-type calcium buffers. Cell Calcium **10:** 491–498

Philippar K, Fuchs I, Luethen H, Hoth S, Bauer CS, Haga K, Thiel G, Ljung K, Sandberg G, Boettger M et al. (1999) Auxin-induced K^+ channel expression represents an essential step in coleoptile growth and gravitropism. Proc Natl Acad Sci USA **96:** 12186–12191

Pilot G, Lacombe B, Gaymard F, Cherel I, Boucherez J, Thibaud JB, Sentenac H (2001) Guard cell inward K^+ channel activity in *Arabidopsis* involves expression of the twin channel subunits KAT1 and KAT2. J Biol Chem **276:** 3215–3221

Racusen R, Satter RL (1975) Rhythmic and phytochrome-regulated changes in transmembrane potential in *Samanea* pulvini. Nature **255:** 408–410

Robinson RA, Stokes RH (1965) Electrolyte Solutions. Butterworths & Co., London

Satter RL, Galston AW (1981) Mechanisms of control of leaf movements. Annu Rev Plant Physiol **32:** 83–110

Satter RL, Moran N (1988) Ionic channels in plant cell membranes. Physiol Plant **72:** 816–820

Schachtman DP, Schroeder JI, Lucas WJ, Anderson JA, Gaber RF (1992) Expression of an inward-rectifying potassium channel by the Arabidopsis KAT1 cDNA. Science **258:** 1654–1658

Schroeder JI (1988) K^+ transport properties of K^+ channels in the plasma membrane of *Vicia faba* guard cells. J Gen Physiol **92:** 667–683

Schroeder JI (1995) Magnesium-independent activation of inward-rectifying K^+ channels in *Vicia faba* guard cells. FEBS Lett **363:** 157–160

Schroeder JI, Hagiwara S (1989) Cytosolic calcium regulates ion channels in the plasma membrane of *Vicia faba* guard cells. Nature **338:** 427–430

Schroeder JI, Raschke K, Neher E (1987) Voltage dependence of K^+ channels in guard-cell protoplasts. Proc Natl Acad Sci USA **84:** 4108–4112

Shimazaki K, Iino M, Zeiger E (1985) Blue light-dependent proton extrusion by guard-cell protoplasts of *Vicia faba*. Nature **319:** 324–326

Starrach N, Meyer W-E (1989) Changes of the apoplastic pH and K^+ concentration in the *Phaseolus* pulvinus in situ in relation to rhythmic leaf movements. J Exp Bot **40:** 865–873

Suh S, Moran N, Lee Y (2000) Blue light activates depolarization-dependent K^+ channels in flexor cells from *Samanea saman* motor organs via two mechanisms. Plant Physiol **123:** 833–843

Szyroki A, Ivashikina N, Dietrich P, Roelfsema MRG, Ache P, Reintanz B, Deeken R, Godde M, Felle H, Steinmeyer R et al. (2001) KAT1 is not essential for stomatal opening. Proc Natl Acad Sci USA **98:** 2917–2921

Tang XD, Marten I, Dietrich P, Ivashikina N, Hedrich R, Hoshi T (2000) Histidine(118) in the S2–S3 linker specifically controls activation of the KAT1 channel expressed in *Xenopus* oocytes. Biophys J **78:** 1255–1269

Uozumi N, Nakamura T, Schroeder JI, Muto S (1998) Determination of transmembrane topology of an inward-rectifying potassium channel from *Arabidopsis thaliana* based on functional expression in *Escherichia coli*. Proc Natl Acad Sci USA **95:** 9773–9778

Very AA, Gaymard F, Bosseux C, Sentenac H, Thibaud JB (1995) Expression of a cloned plant K^+ channel in *Xenopus* oocytes: analysis of macroscopic currents. Plant J **7:** 321–332

Wu WH, Assmann SM (1994) A membrane-delimited pathway of G-protein regulation of the guard-cell inward K^+ channel. Proc Natl Acad Sci USA **91:** 6310–6314

Zei PC, Aldrich RW (1998) Voltage-dependent gating of single wild-type and S4 mutant KAT1 inward rectifier potassium channels. J Gen Physiol **112:** 679–713

Zimmermann S, Sentenac H (1999) Plant ion channels: from molecular structures to physiological functions. Curr Opin Plant Biol **2:** 477–482